

# LARGE-EDDY SIMULATION OF ROTATING TURBULENT CHANNEL FLOW

**N. Alkishriwi, M. Meinke, W. Schröder**

Institute of Aerodynamics, RWTH Aachen University, Aachen, Germany

Email: N.Alkishriwi@aia.rwth-aachen.de

## ABSTRACT

*In many engineering and industrial applications the investigation of rotating turbulent flow is of great interest. In this type of flow the Coriolis force has a strong influence on the turbulence. Turbulent flows in a rotating channel are severely affected by this force, which is induced by the system rotation and produces a secondary flow in the spanwise direction. Some research has been done concerning channel flows with a spanwise rotation axis [1], [2]. However, so far very few investigations have been done on channel flows with a rotation about the streamwise axis [3]. In the present study an LES of a turbulent streamwise rotating channel flow at  $Re_\tau = 180$  is performed using a moving grid method to predict the overall three-dimensional structures and the details of the secondary flow distribution.*

## INTRODUCTION

The simulation of rotating turbulent flow is a major issue in computational fluid dynamics and engineering applications such as in gas turbine blade passages, pumps, and rotating heat exchangers. A few investigations have been done on channel flows with a rotation about the streamwise axis. Analyses of this type of flow based on Lie-group theory and DNS [3] show that a secondary flow perpendicular to the main flow direction is generated whose distribution strongly depends on the rotational speed. Also, the experimental investigations on this type of the flow [4] evidence the existence of the secondary flow in the spanwise direction.

In this study the effects of streamwise rotation on the large-scale structures in a turbulent channel flow are numerically simulated using large-eddy simulations. The investigation is based on the same physical parameters and dimensions as used in the experiment [4] to make sure that a

thorough comparison between experimental and numerical results can be performed. It has to be emphasized that unlike other computations the full spanwise extension of the rotating channel is resolved to avoid the specification of periodic boundary conditions in the spanwise direction. In doing so, the impact of imposing such a spanwise boundary condition, as is usually done in the literature, on the secondary flow field can be analyzed. It is the main purpose of this investigation to shed some light on this question.

## METHOD OF SOLUTION

The large-eddy simulation is based on a finite volume method to approximately solve the three-dimensional compressible Navier-Stokes equations. The LES is carried out using the monotone integrated LES (MILES) approach [5] to represent the effect of non-resolved subgrid scales. In implicitly filtered LES, the computational grid and the discretization operators are considered

as the filtering of the governing equations. A second-order 5-step Runge-Kutta method is used to propagate the solution from time level  $n$  to  $n+1$ . The governing equations are discretized using a second-order accurate modified AUSM (Adjective Upstream Splitting Method) scheme, which possesses a centered 5-point low dissipation stencil to compute the pressure derivative in the convective fluxes. This scheme is described in detail and validated against several test problems such as channel, jet, and pipe flows in [6]. The method is formulated for multi-block structured curvilinear grids and implemented on vector and parallel computers. The viscous stresses are approximated to second-order accuracy using central differences, i.e., the overall spatial approximation is second-order accurate. To enable an efficient analysis even in the low Mach number regime a preconditioned LES method has been developed [7].

The boundary conditions consist of no-slip and isothermal conditions on the walls. In the streamwise direction the pressure and temperature fluctuations and the mass flow are assumed to be periodic. Using the relation  $Re_\tau = 0.1097 Re_{cl}^{0.911}$  from Hussain and Reynolds [9] the pressure difference  $\delta P = 2\rho u_\tau^2 L/H$  that drives the flow is determined by the maximum velocity. The quantity  $u_\tau$  is the friction velocity,  $H$  is the height of the channel, and  $L$  represents the streamwise extent of the channel. The pressure gradient is held constant for all computations.

In this analysis the size of the computational domain in the streamwise  $x$ , spanwise  $z$ , and normal  $y$  direction is given by  $L = 25\delta$ ,  $B = 20\delta$ , and  $H = 2\delta$ . Note, the quantity  $\delta$  is the channel half width, which agrees with the experimental value. We consider turbulent channel flow at a Reynolds  $Re_\tau = 180$ . The simulations are carried out at rotation rates of  $f = 0$  Hz,  $f = 0.46$  Hz, and  $f = 0.8$  Hz corresponding to Rossby numbers  $Ro = \frac{u_b}{\delta f}$  with  $u_b$  being the bulk velocity  $Ro = \infty$ ,  $Ro = 65.2$ , and  $Ro = 37.5$ .

After a fully developed turbulent channel flow has been established the simulations are run for another 700 dimensionless time units in which samples are stored each quarter of a dimensionless time unit. Additionally, the results are averaged in the streamwise and spanwise direction, where only the region  $-\delta < z < \delta$  is considered.

## RESULTS

First, the method of solution has been applied to compute the flow in a stationary channel ( $Ro = \infty$ ) at the same Reynolds number and with the same grid distribution as for the rotating case. The turbulent statistics and the mean flow profiles are compared with the direct numerical simulations of the non-rotating case of Kim et al. [8] and LES results from [10]. Figs. 1 and 2 show the comparison of the distribution of the streamwise, spanwise, normal, and Reynolds shear stresses with DNS and LES data. The present LES results compare well with the DNS results, although some improvement in the distribution of the normal fluctuations is desirable.

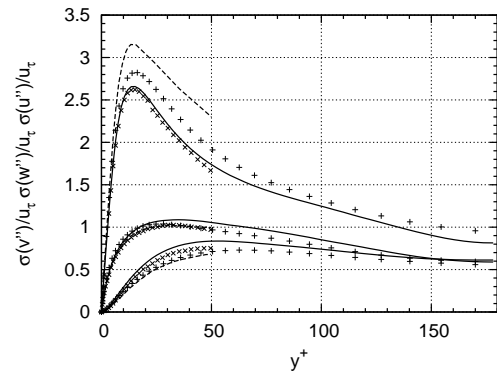


Fig. 1. Comparison of the distribution of the streamwise, spanwise, and normal Reynolds stresses; — DNS data; + present LES; × filtered DNS data; --- LES from [10]

The results of the rotating cases at  $Ro = 65.2$  and  $Ro = 37.5$  are presented in Figs. 3-11. In Fig. 3 the streamwise mean velocity profiles at  $Ro = \infty$ ,  $Ro = 65.2$  and  $Ro = 37.5$  are compared with the

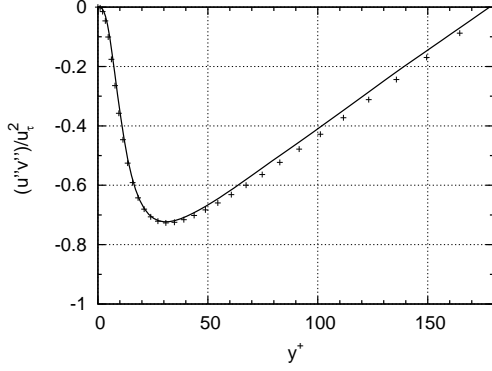


Fig. 2. Comparison of the distribution of the Reynolds shear stresses; — DNS data; + present LES

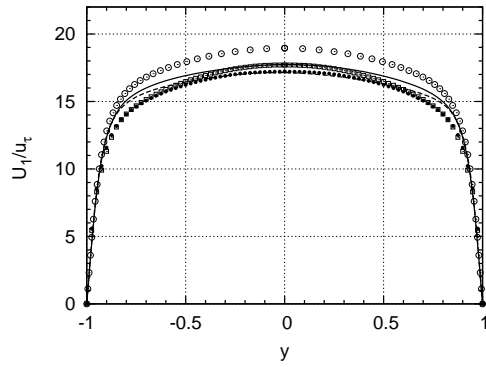


Fig. 3. Streamwise mean velocity profiles at  $Re_\tau = 180$ ;  $\odot$  LES at  $Ro = \infty$ ; — present LES at  $Ro = 65.2$ ; - - - present LES at  $Ro = 37.5$ ;  $\bullet$  exp. data at  $Ro = 65.2$ ;  $\square$  exp. data at  $Ro = 37.5$

experimental data from [4]. A visible change in the mean velocity profiles in the core region of the flow, i.e.,  $-0.5 \leq y \leq 0.5$  due to the increase of the angular velocity is evident. To be more precise, the experimental and numerical data show the larger the rotation speed, the smaller the peak value of the mean streamwise velocity. The distribution of the mean axial velocity shows the main discrepancy in the region  $0.75 < y < 0.85$ . This is likely to be caused by too less measurement data in the near wall region due to seeding problems in the PIV measurements.

As mentioned before, a mean cross flow in the spanwise direction is induced by the rotation. This is shown in Fig. 4. The spanwise velocity distribution possesses only a very weak S-like shape in the vicinity of the symmetry plane. This

agrees with the experiments in [4]. The comparison with the experimental data evidences that this weak secondary motion near the symmetry plane is not captured by the measurements. The reason is that the magnitude of the secondary flow is in the range of the measurement accuracy of the experimental set-up. In other words, the measurements could not resolve this very susceptible structure of the flow field. Nevertheless, there is analytical evidence for the existence of such a flow pattern [3]. However, the analysis in [3] gives only the qualitative distribution, not the quantitative velocity profile. Preliminary results of large-eddy simulations based on spanwise periodic boundary conditions in Fig. 5 indicate that the same flow structure and likewise local peak values develop as in the full spanwise extension of channel simulation, i.e., by taking into account the solid walls in the spanwise directions, presented in Fig. 4. The DNS data [11] shown in Fig. 5 have a much larger secondary motion near the symmetry  $y=0$ . Note that the DNS Rossby numbers  $Ro = 52$  and  $Ro = 104$  are different from the LES solution. However, it is reasonable to assume the DNS solution for  $Ro = 65.2$  to lie between the  $Ro = 52$  and  $Ro = 104$  solutions depicted in Fig. 5. It is conjectured that the discrepancy between the LES and DNS results as to the peak values of the secondary flow is mainly due to the much smaller spanwise extent of the DNS domain. The DNS mesh covers approximately just 1/4 of the LES domain.

From the statistical evaluation the distributions of the streamwise, normal, and spanwise Reynolds stresses are plotted in Figs. 6, 7, and 8. It is clear that all statistical curves are symmetric about the centerline. Unlike the streamwise Reynolds stress  $\overline{u'u'}$  the normal and spanwise Reynolds stresses  $\overline{v'v'}$ ,  $\overline{w'w'}$  are increasing at increasing rotational speed. The distributions indicate a slight growth in the turbulence intensity near the symmetry plane  $y=0$ . In Figs. 9, 10, and 11 the Reynolds shear stresses components possess due to the rotational speed a non-zero distribution. Further-

more, it is evident that the difference in the profiles due to the changing rotational speed are primarily caused by the spanwise component.

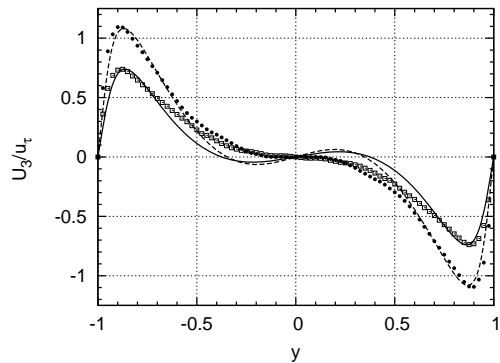


Fig. 4. Spanwise velocity distribution at  $Re_\tau = 180$ ; — present LES at  $Ro = 65.2$ ; - - - present LES at  $Ro = 37.5$ ; • exp. data at  $Ro = 65.2$ ; □ exp. data at  $Ro = 37.5$

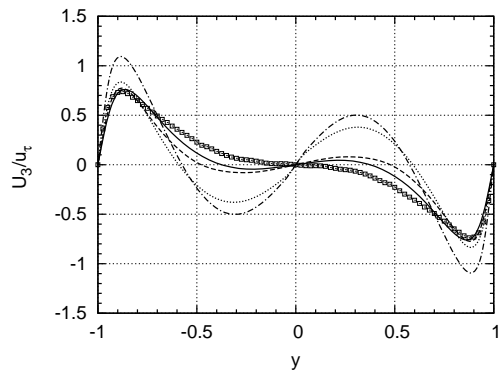


Fig. 5. Spanwise velocity distribution at  $Re_\tau = 180$ ; — present LES at  $Ro = 65.2$  with full spanwise extension; - - - present LES at  $Ro = 65.2$  with a periodic boundary conditions in the spanwise direction; ····· DNS at  $Ro = 104$  from [11]; - · - · - DNS at  $Ro = 52$  from [11]

## CONCLUSIONS

Large-eddy simulations of a turbulent streamwise rotating channel flow at  $Re_\tau = 180$  are performed using a moving grid method to predict the overall three-dimensional structures and the details of the secondary flow distribution. The results confirmed the existence of a secondary flow that has been derived in the literature. This distribution of

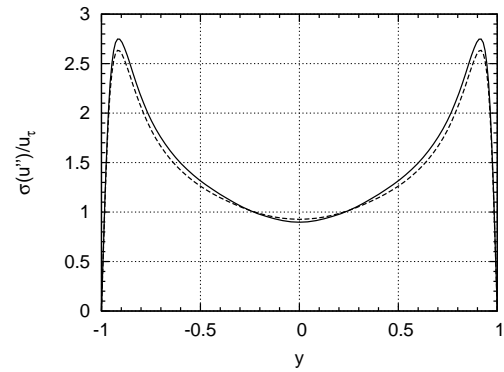


Fig. 6. Distribution of the streamwise Reynolds stresses at  $Re_\tau = 180$ ; — present LES at  $Ro = 65.2$ ; - - - present LES at  $Ro = 37.5$

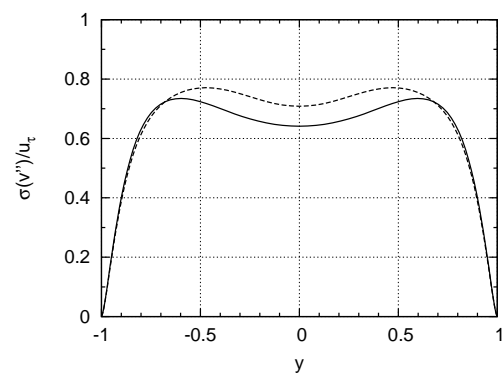


Fig. 7. Distribution of the normal Reynolds stresses at  $Re_\tau = 180$ ; — present LES at  $Ro = 65.2$ ; - - - present LES at  $Ro = 37.5$

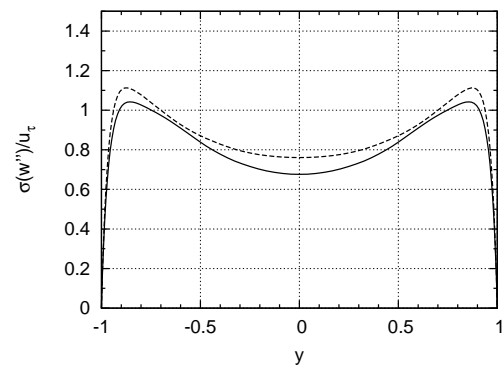


Fig. 8. Distribution of the spanwise Reynolds stresses at  $Re_\tau = 180$ ; — present LES at  $Ro = 65.2$ ; - - - present LES at  $Ro = 37.5$

the secondary flow is independent of the spanwise boundary condition formulation provided the spanwise extent of the computational domain is in the order of  $10\delta$ .

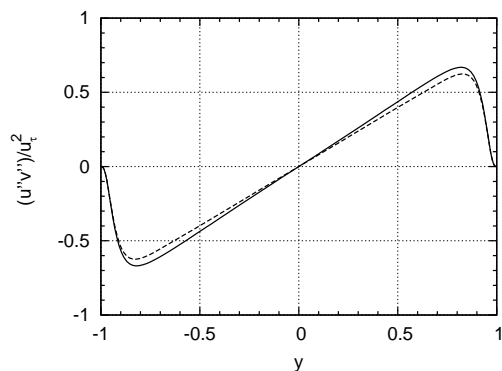


Fig. 9. Distribution of the Reynolds shear stresses  $\overline{u''v''}$  at  $Re_\tau = 180$ ; — present LES at  $Ro = 65.2$ ; - - - present LES at  $Ro = 37.5$

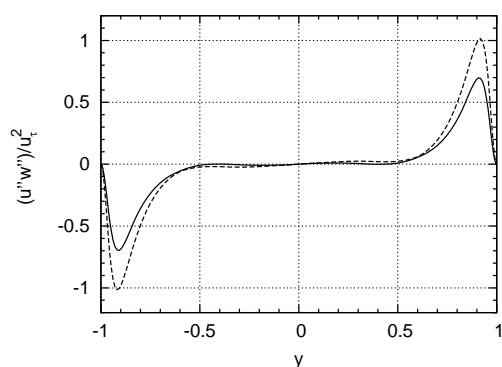


Fig. 10. Distribution of the Reynolds shear stresses  $\overline{u''w''}$  at  $Re_\tau = 180$ ; — present LES at  $Ro = 65.2$ ; - - - present LES at  $Ro = 37.5$

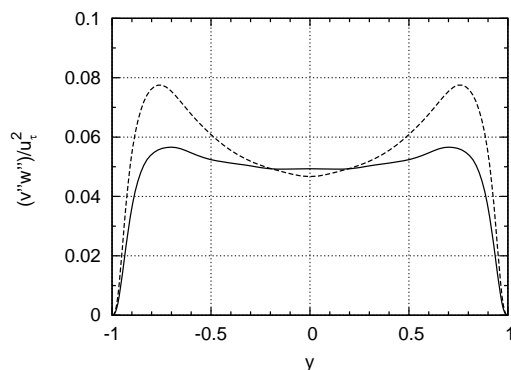


Fig. 11. Distribution of the Reynolds shear stresses  $\overline{v''w''}$  at  $Re_\tau = 180$ ; — present LES at  $Ro = 65.2$ ; - - - present LES at  $Ro = 37.5$

## BIBLIOGRAPHY

[1] R. Kristofferson, H.I. Andersson, "Direct Simulations of Low Reynolds Number Turbulent

Flow in a Rotating Channel," J. Fluid Mech. 256, pp. 163-197, 1993.

[2] E. Lamballais, O. Metais, "Effect of Spanwise Rotation on the Vorticity Stretching in Transitional and Turbulent Channel Flow," Int. J. Heat and Fluid Flow 17, (3), PP. 325-332, 1996.

[3] M. Oberlack, W. Cabot, M.M. Rogers, "Group Analysis, DNS and Modelling of Turbulent Channel Flow with Streamwise Rotation," Center for turbulence research, Proceedings of the summer Programm, pp. 221-242, 1998.

[4] I. Recktenwald, Ch. Brücker, W. Schröder, "PIV investigations of a turbulent channel flow rotating about the streamwise axis," Proceedings of the Tenth European Turbulence Conference, Trondheim, Norway, 2004.

[5] J.P. Boris, F.F. Grinstein, E.S. Oran, R.L. Kolbe, "New insights into large eddy simulation," Fluid Dynamics Research, Vol. 10 (1992).

[6] M. Meinke, W. Schröder, E. Krause, T. Rister, "A comparison of second- and sixth-order methods for large-eddy simulations," Comp. & Fluids, Vol. 31, pp. 695-718, 2002.

[7] N. Alkishriwi, M. Meinke, W. Schröder, "A large-eddy simulation method for low Mach number flows using preconditioning and multigrid," Comp. & Fluids, in press, 2005.

[8] J. Kim, P. Moin, R.D. Moser, "Turbulent statistics in fully developed channel at low Reynolds number," J. Fluid Mech. 177,133-166, 1987.

[9] A.K. Hussain, W.C. Reynolds, "Measurement in fully developed turbulent channel flow," Trans. ASME, pp. 568-580, 1975.

[10] M. Germano, U. Piomelli, P. Moin, W. Cabot, "A Dynamic Subgrid-Scale Eddy Viscosity Model," J. Phys. of Fluids, A 3(7), pp. 1760-1765, 1991.

[11] T. Weller, M. Oberlack, I. Recktenwald, W. Schröder, "DNS and Experiment of a Turbulent Channel Flow with Streamwise Rotation-Study of the Cross Flow Phenomenal," Proc. Appl. Math. Mech. 5, pp. 569-579, 2005.